Small-signal modeling and optimal operating condition of magnetostrictive energy harvester

Journal of Magnetism and Magnetic Materials 547 (2022) 168819

Contents lists available at ScienceDirect

Journal of Magnetism and Magnetic Materials

journal homepage: www.elsevier.com/locate/jmmm

Research articles

Small-signal modeling and optimal operating condition of magnetostrictive energy harvester

Yoshito Mizukawa [a,*], Umair Ahmed [a], Mauro Zucca [b], David Blažević [a], Paavo Rasilo [a]

[a] Tampere University, Electrical Engineering, Korkeakoulunkatu 3, Tampere, Finland
[b] Istituto Nazionale di Ricerca Metrologica, INRIM, Strada delle Cacce 91, Torino, Italy

ARTICLE INFO

Keywords:
Energy harvesting
Linearized modeling
Magnetostriction
Optimization
Parameter variation

ABSTRACT

Magnetostrictive energy harvesting has drawn attention in recent years for its high energy conversion efficiency and environmental durability. Magnetostrictive harvesters are mainly composed of giant magnetostrictive material, a magnetic circuit, and an electric circuit, which involves complex mechanical-electromagnetic coupled problems. Therefore, in many studies, the analysis of such device was implemented by finite element method. However, numerical calculation generally requires a great deal of time and does not provide adequate physical understanding of the effect of the design parameters on the harvester characteristics.

In many previous studies, magnetostrictive harvesters have been operated under a small-signal vibration imposed over a constant prestress and magnetic bias. In such operating conditions, linearized small-signal models can be used to derive important analytical expressions for the harvester characteristics and their dependency on the design parameters. This paper presents the linearized modeling of a magnetostrictive energy harvester using linearized constitutive equations. The energy loss due to eddy currents is also considered for high-frequency application. The influence of parameter variation on the output power is investigated from the algebraically obtained output power, and the existence of an optimal value in resistance and capacitance of the electric circuit is discussed. These optimal design parameters are also presented in form of an algebraic solution. The obtained output power is finally proven to fit with experimental results when an appropriate permeability and magnetostrictive constant are given.

1. Introduction

Energy harvesting technologies have been studied as a solution for supplying autonomous power for wireless sensor networks [1] and Internet of Things applications [2] in which costs of periodic battery replacement and environmental issues by battery disposal are of great concern. Vibration energy harvesting devices offer a great advantage in their wide range of applications compared to devices utilizing other ambient energy sources. In addition, they can also be attached as a vibration suppression device for machine structures [3,4] thus serving as a multifunctional device. For energy harvesting purposes, electromagnetic induction and piezoelectric effect are the most common methods for converting kinetic energy of vibrations to electrical energy.

Piezoelectric energy harvesters have been investigated in various studies due to their high energy density and simple device structure. Ottman et al. [5] presented an adaptive piezoelectric energy harvesting device and maximized the output power flowing into a battery. Soltani et al. [6] optimized the device as a vibration absorber. The resonant amplitude of the host structure derived from linear piezoelectric constitutive equations was minimized using fixed-point theory [7] and Nishihara's method [8]. Yamada [9] proposed a method to enhance the efficiency of a piezoelectric element based on mechanical impedance matching. However, the piezoelectric element is a ceramic material and it cannot be used in applications involving large mechanical inputs or long-term usage. Therefore, the instability of piezoelectric energy harvesters has been discussed [10].

Magnetostrictive energy harvesting is a novel power generation method based on magnetic induction which utilizes the Joule and Villari effects present in giant magnetostrictive materials to convert between strain energy and magnetic energy. Joule effect refers to the deformation of ferromagnetic materials when subject to magnetic fields and this effect is also known as magnetostriction. On the other hand, Villari effect refers to the change of magnetic properties under applied mechanical stress, and it is also known as inverse magnetostriction. Fe-Ga alloy (Fe 81.6%, Ga 18.4%) is one of giant magnetostrictive materials, and it is renowned for its high energy conversion efficiency, low hysteresis loss and environmental durability [11,12]. In addition, the

* Corresponding author.
E-mail address: yoshito.mizukawa@tuni.fi (Y. Mizukawa).

https://doi.org/10.1016/j.jmmm.2021.168819
Received 28 January 2021; Received in revised form 15 August 2021; Accepted 10 November 2021
Available online 4 December 2021

high tensile strength and machinability of Fe-Ga alloy facilitate mass manufacturing of magnetostrictive energy harvesting devices [13].

Regarding the potential output power of magnetostrictive energy harvesters, several studies have been conducted experimentally and numerically. Palumbo et al. [14] focused on the change of magnetostrictive properties under different mechanical prestress and magnetic bias, and experimentally investigated the effect of parameter variations. The optimal operating condition and its output power were obtained from the experiments. The obtained output power and induced voltage were interpolated by exponential fit. Davino et al. [15] proposed a finite element method (FEM) eddy current model for a magnetostrictive energy harvester, where the nonlinear static characteristic of the material is considered. The obtained power versus frequency curves clearly represent the energy damping due to eddy current effect. Ahmed et al. [16,17] conducted FEM analyses of a magnetostrictive energy harvester including magnetic and electric circuits based on the Helmholtz free energy density function. The results fairly agree with experimental data, and the existence of the optimal design parameter and optimal operating condition were finally discussed in the conclusion. However, these kinds of numerical calculations generally require a great deal of time and computational cost, hence an alternative analytical modeling tool in which the characteristics of magnetostrictive energy harvesters can be reasonably described is also needed. In this paper, we develop an analytical linear model for a Fe-Ga energy harvester based on the linearized magnetostrictive constitutive equations. The linearized approach is effective when the mechanical variations are sufficiently small [18–21]. The harvester is assumed to be operated under a considerably low frequency force excitation compared to its natural frequency. The eddy current loss is also taken into account under the assumption that the magnetic flux density is uniform with regards to the cross section of the Fe-Ga rod. From the derived output power, we investigate the effects of parameter variation and the optimal operating condition.

2. Small signal models

2.1. Constitutive equations

The magnetostrictive constitutive equations linearized for small-signal behavior are given as follows [20]:

$$\left.\begin{aligned} \Delta \boldsymbol{B} &= \left[\mu^{\mathrm{T}}\right] \Delta \boldsymbol{H} + [d]^{*}\, \Delta \boldsymbol{T} \\ \Delta \boldsymbol{S} &= [d]\, \Delta \boldsymbol{H} + \left[s^{\mathrm{H}}\right] \Delta \boldsymbol{T} \end{aligned}\right\} \tag{1}$$

where $\boldsymbol{B}$, $\boldsymbol{H}$, $\boldsymbol{S}$, and $\boldsymbol{T}$ are the magnetic flux density, magnetic field strength, mechanical strain and mechanical stress, respectively. The small variation of the quantities is denoted by Δ. $\left[\mu^{\mathrm{T}}\right]$ is the permeability matrix at constant stress, $\left[s^{\mathrm{H}}\right]$ is the elastic compliance matrix at constant magnetic strength, $[d]^{*}$ is the transpose of the magnetostrictive constant matrix $[d]$. In this study, we analyze the Fe-Ga energy harvester shown in Fig. 1. In this case, we consider only the longitudinal direction where mechanical force is applied, and thus (1) can be represented as 1D constitutive equations:

$$\begin{Bmatrix} \Delta B \\ \Delta S \end{Bmatrix} = \begin{bmatrix} \mu^{\mathrm{T}} & d \\ d & s^{\mathrm{H}} \end{bmatrix} \begin{Bmatrix} \Delta H \\ \Delta T \end{Bmatrix} \tag{2}$$

Equation (2) can be transformed by multiplying with the cross-sectional area A and the length l of the Fe-Ga rod.

$$\begin{Bmatrix} \Delta \phi \\ \Delta x \end{Bmatrix} = \begin{bmatrix} \dfrac{1}{R_{\mathrm{FeGa}}} & d \\ d & \dfrac{1}{k_{\mathrm{FeGa}}} \end{bmatrix} \begin{Bmatrix} \Delta F_{\mathrm{FeGa}} \\ \Delta f_{\mathrm{FeGa}} \end{Bmatrix} \tag{3}$$

where ϕ and x are the magnetic flux and displacement, respectively. R_{FeGa}, k_{FeGa}, F_{FeGa}, and f_{FeGa} respectively are the magnetic reluctance,

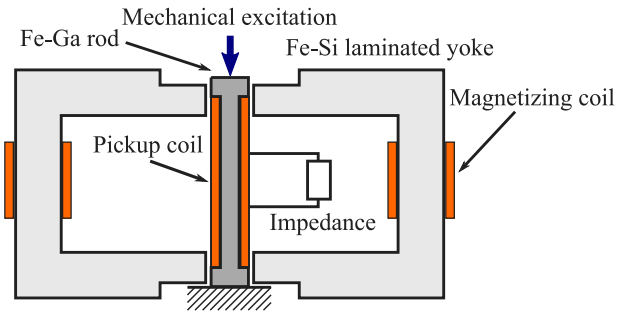

Fig. 1. Schematic diagram of Fe-Ga energy harvester.

spring constant, magnetomotive force, and mechanical force of the Fe-Ga rod. By multiplying the inverse of the coefficient matrix from the left, we can solve (3) with regards to F_{FeGa} and f_{FeGa}:

$$\begin{Bmatrix} \Delta F_{\mathrm{FeGa}} \\ \Delta f_{\mathrm{FeGa}} \end{Bmatrix} = \begin{bmatrix} \overline{R_{\mathrm{FeGa}}} & -\theta \\ -\theta & \overline{k_{\mathrm{FeGa}}} \end{bmatrix} \begin{Bmatrix} \Delta \phi \\ \Delta x \end{Bmatrix} \tag{4}$$

where

$$\left.\begin{aligned} \overline{R_{\mathrm{FeGa}}} &= \frac{R_{\mathrm{FeGa}}}{1-k_0^2} \\ \overline{k_{\mathrm{FeGa}}} &= \frac{k_{\mathrm{FeGa}}}{1-k_0^2} \\ \theta &= k_0 \sqrt{\overline{R_{\mathrm{FeGa}}}\ \overline{k_{\mathrm{FeGa}}}} = d\, R_{\mathrm{FeGa}}\ \overline{k_{\mathrm{FeGa}}} \end{aligned}\right\} \tag{5}$$

$$k_0 = \frac{d}{\sqrt{\mu^{\mathrm{T}} s^{\mathrm{H}}}} \tag{6}$$

k_0 is the value known as magnetostrictive coupling coefficient. This coefficient represents the energy conversion efficiency between mechanical energy and magnetic energy, and ranges from 0 to 1.

2.2. Eddy current effects

In general, magnetic flux change in a conducting material induces an eddy current inside of the material. This eddy current generates a magnetic field acting against the magnetic flux change and causes energy loss in the system. The analytical modeling of this energy loss can generally be derived by solving the 1D axisymmetric magnetic diffusion equation as a 0-order Bessel equation, and it is known that the solution takes a form of infinite series [22,23]. In this section, we analytically derive the opposing magnetic field from the eddy current with the assumption that the magnetic flux density is uniform with regards to cross-sectional area of the Fe-Ga rod.

The 1D axisymmetric magnetic diffusion equation with the assumption of uniform magnetic flux density is given as follows:

$$\frac{1}{r}\frac{\partial}{\partial r}\left(r\frac{\partial H_{\mathrm{ed}}(r,t)}{\partial r}\right) = \sigma \dot{B}(t) \tag{7}$$

where r, H_{ed}, t, and σ are the radial coordinate, magnetic field by eddy current, time, and conductivity of Fe-Ga alloy, respectively. Solving (7) gives the solution:

$$H_{\mathrm{ed}}(r,t) = \frac{1}{4}\sigma r^2 \dot{B}(t) + c_1 \ln r + c_2 \tag{8}$$

where c_1 and c_2 are integral constants determined by boundary conditions. The first boundary condition can be obtained from the condition that (8) should have a finite value at $r = 0$, and the second boundary condition can be obtained from the condition that the H_{ed} should be

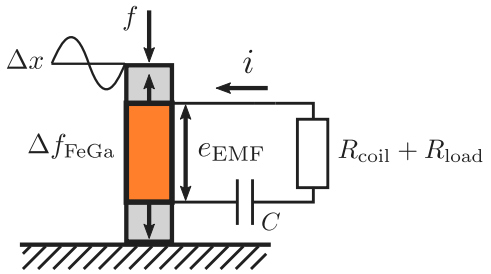

Fig. 2. Analytical model of Fe-Ga rod with electric circuit.

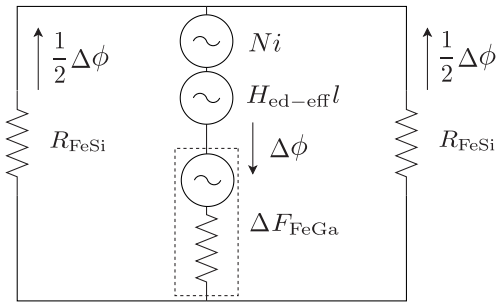

Fig. 3. Dynamic magnetic circuit diagram.

zero at the surface of the Fe-Ga rod. These boundary conditions give

$$\left.\begin{aligned} c_1 &= 0 \\ c_2 &= -\frac{1}{4}\sigma R^2 \dot{B}(t) \end{aligned}\right\} \tag{9}$$

$$H_{\mathrm{ed}}(r,t) = \frac{1}{4}\sigma r^2 \dot{B}(t) - \frac{1}{4}\sigma R^2 \dot{B}(t) \tag{10}$$

where R is the radius of the Fe-Ga rod. Here, we define the average of (10) as the effective reaction field caused by the eddy currents:

$$H_{\mathrm{ed-eff}}(t) = \frac{1}{\pi R^2}\int_A H_{\mathrm{ed}}(r,t)\mathrm{d}A = \frac{2}{R^2}\int_0^R H_{\mathrm{ed}}(r,t) r \mathrm{d}r \tag{11}$$

which simplifies to

$$H_{\mathrm{ed-eff}}(t) = -\frac{1}{8}\sigma R^2 \dot{B}(t) = -\frac{1}{8\pi}\sigma\dot{\phi}(t) \tag{12}$$

2.3. System model

In this section, we derive the system of equations for the magnetostrictive energy harvester in which the equation of motion, magnetic circuit equation, and electric circuit equation are coupled. The following assumptions are applied to the equations: (i) inertia force of the Fe-Ga rod is negligible because the natural frequency of the rod is much higher than the operating frequency band, (ii) leakage flux from the magnetic circuit is negligible and (iii) leakage inductance of the pickup coil is small enough to be neglected.

Fig. 2 shows the analytical model of the Fe-Ga rod with the pickup coil connected to an electric circuit with a load resistor and a compensating capacitor. When dynamic mechanical force f is applied to the Fe-Ga rod, an electromotive force e_{EMF} is generated in the pickup coil since the flux linkage changes due to inverse magnetostriction. On the other hand, the induced current i flowing through the pickup coil causes the mechanical deformation with force Δf_{FeGa} by magnetostriction. These phenomena give the equation of motion:

$$\Delta f_{\mathrm{FeGa}} - f = 0 \tag{13}$$

and electric circuit equation:

$$e_{\mathrm{EMF}} = \left(R_{\mathrm{coil}} + R_{\mathrm{load}}\right) i + \frac{1}{C}\int i\mathrm{d}t \tag{14}$$

where R_{coil} and R_{load} respectively are the resistance of the pickup coil and load resistor. C is the capacitance of the compensating capacitor. By applying Faraday's law,

$$e_{\mathrm{EMF}} = -N\dot{\phi} \tag{15}$$

(14) can be represented with the number of turns of pickup coil N and time-derivative of magnetic flux $\dot{\phi}$:

$$N\dot{\phi} + \left(R_{\mathrm{coil}} + R_{\mathrm{load}}\right) i + \frac{1}{C}\int i\mathrm{d}t = 0 \tag{16}$$

The dynamic magnetic circuit diagram shown in Fig. 3 gives the following magnetic circuit equation:

$$\Delta F_{\mathrm{FeGa}} - Ni - H_{\mathrm{ed-eff}} l + \frac{1}{2} R_{\mathrm{FeSi}} \Delta\phi = 0 \tag{17}$$

where R_{FeSi} is the magnetic reluctance of the Fe-Si laminated yoke. By assigning (4) and (12) to (13), (16), and (17), we can finally obtain the system of equations for the Fe-Ga energy harvester:

$$\left.\begin{aligned} &\overline{k_{\mathrm{FeGa}}} x - \theta\phi - f = 0 \\ &\overline{R_{\mathrm{FeGa}}}\phi - \theta x - Ni + \frac{1}{8\pi}\sigma l\dot{\phi} + \frac{1}{2}R_{\mathrm{FeSi}}\phi = 0 \\ &N\dot{\phi} + \left(R_{\mathrm{coil}} + R_{\mathrm{load}}\right) i + \frac{1}{C}\int i\mathrm{d}t = 0 \end{aligned}\right\} \tag{18}$$

where the small signal symbol Δ was omitted for convenience. Solving (18) gives the harmonic solutions:

$$\left.\begin{aligned} x &= \frac{\alpha_x + j\beta_x}{\alpha + j\beta}\frac{f}{\overline{k_{\mathrm{FeGa}}}} \\ \phi &= \frac{\alpha_\phi + j\beta_\phi}{\alpha + j\beta} f \\ i &= \frac{\alpha_i}{\alpha + j\beta} f \end{aligned}\right\} \tag{19}$$

$$\left.\begin{aligned} \alpha =& 8\pi\omega^2 N^2 + \omega^2\sigma l\left(R_{\mathrm{coil}} + R_{\mathrm{load}}\right) \\ &- \frac{4\pi}{C}\left(R_{\mathrm{FeSi}} + 2R_{\mathrm{FeGa}}\right) \\ \beta =& -4\pi\omega\left(R_{\mathrm{FeSi}} + 2R_{\mathrm{FeGa}}\right)\left(R_{\mathrm{coil}} + R_{\mathrm{load}}\right) \\ &- \frac{1}{C}\omega\sigma l \\ \alpha_x =& 8\pi\omega^2 N^2 + \omega^2\sigma l\left(R_{\mathrm{coil}} + R_{\mathrm{load}}\right) \\ &- \frac{4\pi}{C}\left(R_{\mathrm{FeSi}} + 2\overline{R_{\mathrm{FeGa}}}\right) \\ \beta_x =& -4\pi\omega\left(R_{\mathrm{FeSi}} + 2\overline{R_{\mathrm{FeGa}}}\right)\left(R_{\mathrm{coil}} + R_{\mathrm{load}}\right) \\ &- \frac{1}{C}\omega\sigma l \\ \alpha_\phi =& -\frac{8\pi}{C} d R_{\mathrm{FeGa}} \\ \beta_\phi =& -8\pi\omega d R_{\mathrm{FeGa}}\left(R_{\mathrm{coil}} + R_{\mathrm{load}}\right) \\ \alpha_i =& -8\pi\omega^2 d N R_{\mathrm{FeGa}} \end{aligned}\right\} \tag{20}$$

where j and ω respectively are the imaginary unit and excitation frequency, and solutions were simplified using (5). Among the solutions in (20), x and i can respectively be utilized for vibration suppression [24] and energy harvesting purposes. The average output power from the load resistance can be obtained as follows:

$$P_{\mathrm{ave}} = \frac{|i|^2 R_{\mathrm{load}}}{2} = \frac{\alpha_i^2 R_{\mathrm{load}}}{2\left(\alpha^2 + \beta^2\right)} f^2 \tag{21}$$

3. Parameter variation effects and optimal operating condition

In this section, we investigate the effects of parameter changes on the average output power. The aim of this investigation is to confirm the agreement of the proposed linear model with the laws of physics, and to find the conditions for high-efficiency magnetostrictive energy harvester. The average output power P_{ave} versus excitation frequency $\omega/2\pi$ curves (Fig. 4), P_{ave} versus load resistance R_{load} curves (Fig. 5), and P_{ave} versus capacitance C curves (Fig. 6) were produced with different values of (a) conductivity σ, (b) permeability μ and (c) magnetostrictive constant d.

In Fig. 4(a), the difference between output powers with different conductivities increases as frequency increases, which reasonably represents the feature of the eddy current loss. In Figs. 4(b) and 4(c), it can be observed that the smaller permeability or higher magnetostrictive constant leads to higher output power, which clearly represents the increment of the magnetostrictive coupling coefficient expressed by (6). It is also noteworthy that all the output power curves in Fig. 4 converge to constant values regardless of σ, μ and d.

In Figs. 5(a)–5(c) and 6(a)–6(c), it is notable that all the curves have a peak value, which means that the magnetostrictive energy harvester has an optimal load resistance and an optimal capacitance at which the maximum output power can be harvested. These optimal design parameters vary when the value of conductivity or permeability changes. On the other hand, they are not affected by the change of the magnetostrictive constant. The optimal load resistance R_{opt} and optimal capacitance C_{opt} can be derived from the following equations:

$$\left.\frac{\partial P_{\text{ave}}}{\partial R_{\text{load}}}\right|_{R_{\text{load}}=R_{\text{opt}}} = 0, \quad \left.\frac{\partial P_{\text{ave}}}{\partial C}\right|_{C=C_{\text{opt}}} = 0 \tag{22}$$

$$\left.\begin{aligned} R_{\text{opt}} &= \frac{8\pi\omega^2\sigma N^2 l}{16\pi^2\left(2R_{\text{FeGa}}+R_{\text{FeSi}}\right)^2+\omega^2\sigma^2 l^2}+R_{\text{coil}} \\ C_{\text{opt}} &= \frac{16\pi^2\left(2R_{\text{FeGa}}+R_{\text{FeSi}}\right)^2+\omega^2\sigma^2 l^2}{32\pi^2\omega^2 N^2\left(2R_{\text{FeGa}}+R_{\text{FeSi}}\right)} \end{aligned}\right\} \tag{23}$$

As seen from (23), we can confirm that both the optimal load resistance R_{opt} and optimal capacitance C_{opt} are independent of magnetostrictive constant d. By substituting the (23) into (21), we can obtain the maximum output power:

$$\left.\begin{aligned} P_{RC\max} = \\ \frac{8\pi^2\omega^2 d^2 N^2 R_{\text{FeGa}}^2 f^2}{\left[16\pi^2\left(2R_{\text{FeGa}}+R_{\text{FeSi}}\right)^2+\omega^2\sigma^2 l^2\right]R_{\text{coil}}+8\pi\omega^2\sigma l N^2} \end{aligned}\right\} \tag{24}$$

For comparison, the optimal resistance and maximum output power for a pure resistance circuit ($C=\infty$) were also calculated:

$$R_{\text{opt}} = \sqrt{\frac{64\pi^2\omega^2 N^4+16\pi\omega^2\sigma l N^2 R_{\text{coil}}}{16\pi^2\left(2R_{\text{FeGa}}+R_{\text{FeSi}}\right)^2+\omega^2\sigma^2 l^2}+R_{\text{coil}}^2} \tag{25}$$

$$P_{R\max} = \frac{16\pi^2\omega^2 d^2 N^2 R_{\text{FeGa}}^2 f^2}{aR_{\text{coil}}+8\pi\omega^2\sigma l N^2+\sqrt{a\left(aR_{\text{coil}}^2+b\right)}} \tag{26}$$

where

$$\left.\begin{aligned} a &= 16\pi^2\left(2R_{\text{FeGa}}+R_{\text{FeSi}}\right)^2+\omega^2\sigma^2 l^2 \\ b &= 16\left(4\pi^2\omega^2 N^4+\pi\omega^2\sigma l N^2 R_{\text{coil}}\right) \end{aligned}\right\} \tag{27}$$

Regardless of the parameters, (24) is greater than (26). Therefore, the optimized harvester with an RC circuit can harvest more electrical power than that with a pure resistance circuit.

The eddy current effect can be reduced by decreasing the effective conductivity σ. The effective conductivity can be decreased by changing from a solid rod to a laminated structure [25] or introducing more complex cross-sectional shapes to increase the resistance encountered by the eddy currents [26]. Fig. 7 shows the output powers increased by reducing the eddy current effect. The power difference between $P_{RC\max}$ and $P_{R\max}$ becomes larger as the effective conductivity decreases. In the case of no effective conductivity ($\sigma=0$), the optimal parameters (23)

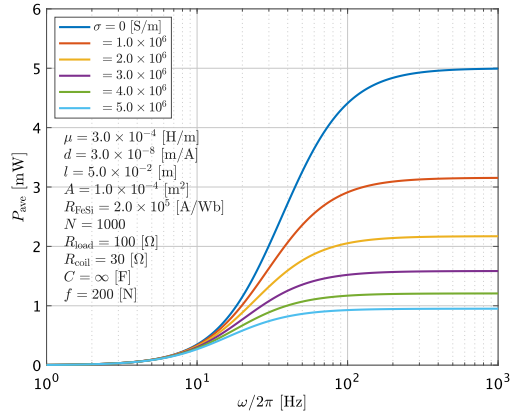

(a) Variation of conductivity σ

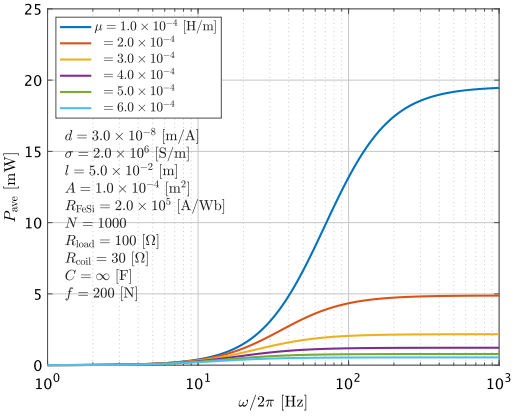

(b) Variation of permeability μ

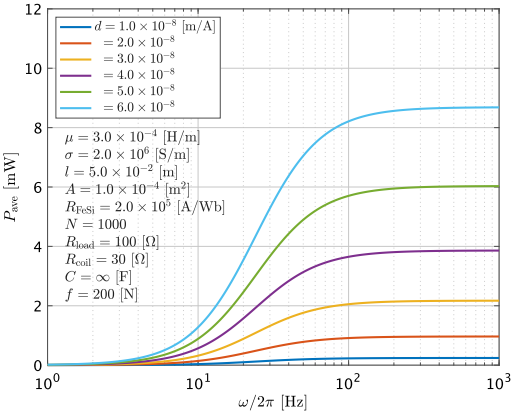

(c) Variation of magnetostrictive constant d

Fig. 4. Parametric study of the output power versus frequency for different conductivities, permeabilities and magnetostrictive constants of the Fe-Ga rod.

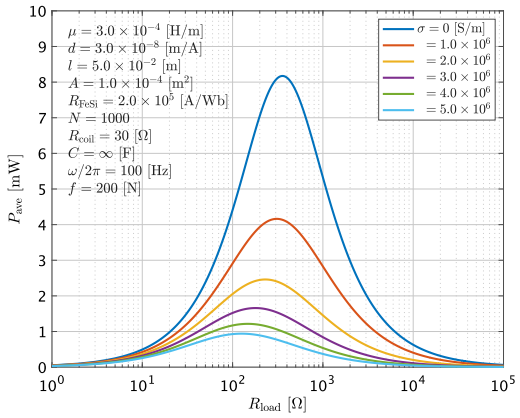

(a) Variation of conductivity σ

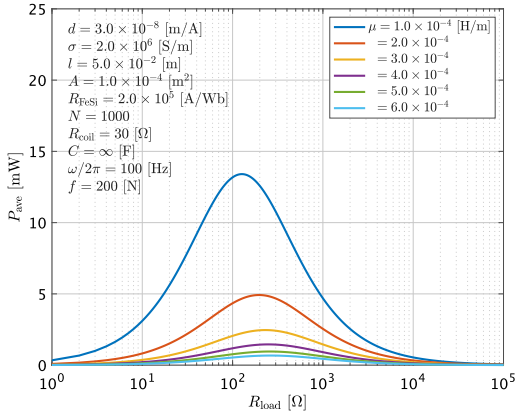

(b) Variation of permeability μ

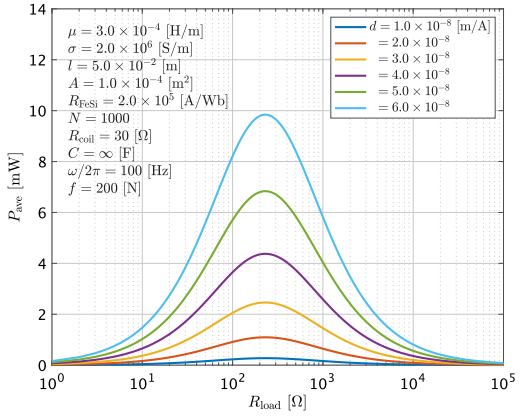

(c) Variation of magnetostrictive constant d

Fig. 5. Parametric study of the output power versus load resistance for different conductivities, permeabilities and magnetostrictive constants of the Fe-Ga rod.

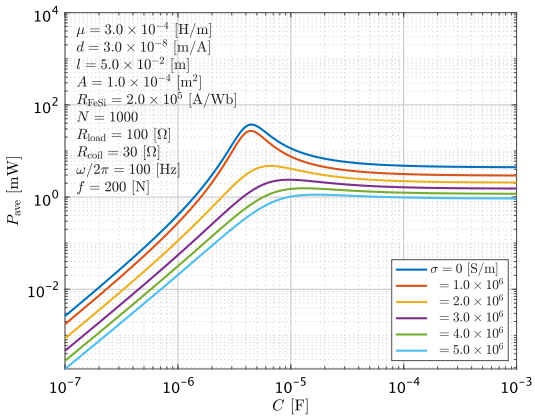

(a) Variation of conductivity σ

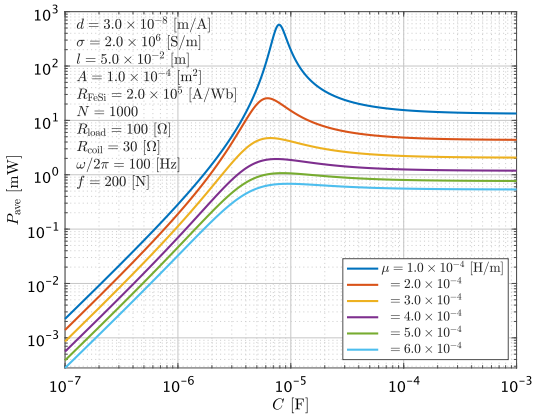

(b) Variation of permeability μ

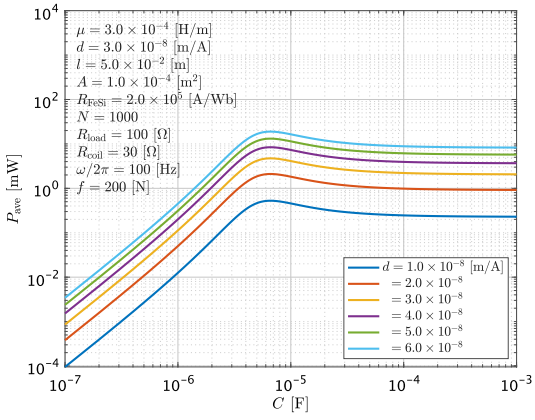

(c) Variation of magnetostrictive constant d

Fig. 6. Parametric study of the output power versus capacitance for different conductivities, permeabilities and magnetostrictive constants of the Fe-Ga rod.

and the maximum output power (24) respectively are

$$\left.\begin{aligned} R_{\mathrm{opt}} &= R_{\mathrm{coil}} \\ C_{\mathrm{opt}} &= \frac{2R_{\mathrm{FeGa}} + R_{\mathrm{FeSi}}}{2\omega^2 N^2} \end{aligned}\right\} \tag{28}$$

$$P_{RC\max} = \frac{\omega^2 d^2 N^2 R_{\mathrm{FeGa}}^2 f^2}{2\left(2R_{\mathrm{FeGa}} + R_{\mathrm{FeSi}}\right)^2 R_{\mathrm{coil}}} \tag{29}$$

The optimal resistance (25) and the maximum output power (26) for the pure resistance circuit respectively are

$$R_{\mathrm{opt}} = \sqrt{\frac{4\omega^2 N^4}{\left(2R_{\mathrm{FeGa}} + R_{\mathrm{FeSi}}\right)^2} + R_{\mathrm{coil}}^2} \tag{30}$$

$$P_{R\max} = \frac{\omega^2 d^2 N^2 R_{\mathrm{FeGa}}^2 f^2}{\left(2R_{\mathrm{FeGa}} + R_{\mathrm{FeSi}}\right)^2 R_{\mathrm{coil}}\left(1 + \sqrt{1 + c^2}\right)} \tag{31}$$

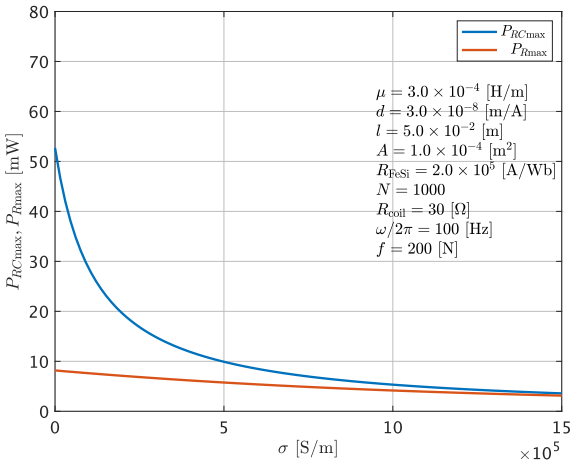

Fig. 7. Reducing eddy current effect by decreasing effective conductivity.

Table 1
Parameters of experimental setup.

Parameter	Definition	Value
σ	Conductivity	1.18×10^6 S/m
l	Rod length	48×10^{-3} m
A	Rod area	2.83×10^{-5} m^2
R_{FeSi}	Reluctance of yoke	1.94×10^5 A/Wb
N	Number of turns	2000
R_{coil}	Resistance of coil	32.6 Ω
f	Excitation force	226 N

where

$$c = \frac{2\omega N^2}{\left(2R_{\mathrm{FeGa}} + R_{\mathrm{FeSi}}\right)^2 R_{\mathrm{coil}}} \tag{32}$$

4. Experiment

Figs. 8(a) and 8(b) display the dimensions of the experimental Fe-Ga energy harvester. The Fe-Ga rod with effective length of 48 mm and effective diameter of 6 mm was connected to the Fe-Si laminated yoke by two pure iron rings. Two sets of series connected coils with 600 turns were utilized to provide the magnetic bias for the Fe-Ga rod. The pick up coil with a load resistance was wrapped around the Fe-Ga rod. The device was mechanically excited by the fatigue-testing machine (Instron, model E10000, Instron Corp., Norwood, MA, USA) which can simultaneously provide a constant mechanical bias and a sinusoidal mechanical force excitation up to 7 kN rms at maximum frequency of 100 Hz. Table 1 shows the parameters of the experimental setup. The rod length l of the harvester was determined by the dimensions of the Fe-Si laminated yoke. The rod area of the harvester was defined by the predetermined excitation force and the required preload which provides the maximum output power [14]. The magnetic reluctance of Fe-Si laminated yoke R_{FeSi} was calculated from its effective length, cross-sectional area, and permeability. In this study, we neglected the magnetic reluctance of the pure iron rings.

The obtained output power P_{ave} was fitted to the experimental results and magnetic constant d and permeability μ which give the best fit with the experimental results were investigated. Fig. 9 shows power versus excitation frequency plots and fitted curves at different excitation amplitudes. In this experiment, a load resistance of $R_{\mathrm{load}} = 160\ \Omega$ was used. The proposed linearized model with $d = 4.38 \times 10^{-8}$ m/A and $\mu = 2.94 \times 10^{-4}$ H/m gives a good agreement with all 3 experimental data in the whole frequency domain.

Fig. 10 shows power versus load resistance plots and fitted curves at different mechanical preloads. Since the magnetostrictive constant d and permeability μ respectively change depending on the value of

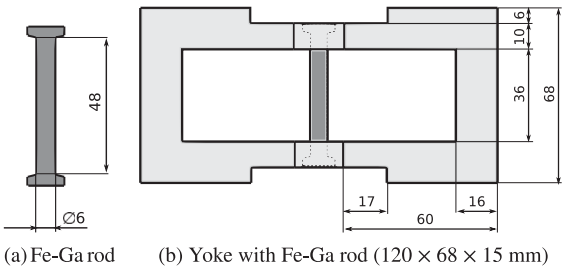

Fig. 8. Dimensions of experimental Fe-Ga energy harvester.

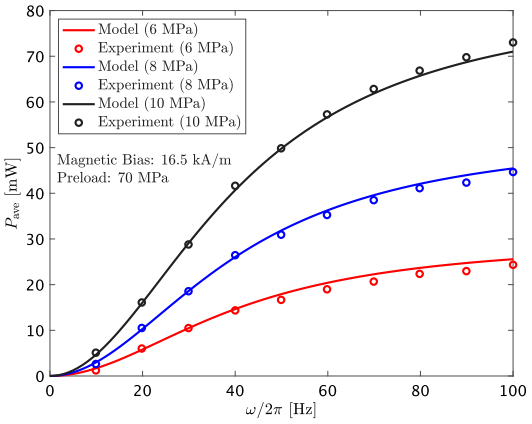

Fig. 9. Experimental results at different excitation amplitude and fitted model in power versus frequency curves ($d = 4.38 \times 10^{-8}$ m/A, $\mu = 2.94 \times 10^{-4}$ H/m).

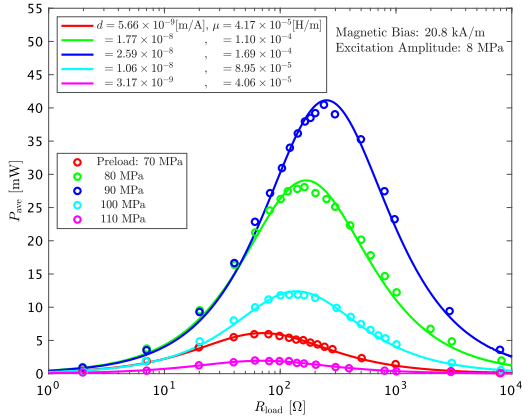

Fig. 10. Experimental results (markers) at different preload and fitted models (solid lines) in power versus resistance curves ($\omega/2\pi = 100$ Hz).

preload, curve fitting was applied to each experimental data with different mechanical preload. As shown in Fig. 10, both the magnetostrictive constant d and permeability μ obtained by the curve fitting increase as the mechanical preload increases from 70 MPa to 90 MPa. After taking the peak value ($d = 2.59 \times 10^{-8}$ m/A and $\mu = 1.69 \times 10^{-4}$ H/m) at 90 MPa, they decrease as the mechanical preload further increases from 90 MPa to 110 MPa.

5. Conclusion

This paper presented a linearized small-signal modeling tool of the magnetostrictive energy harvester which can reasonably represent the characteristics of the magnetostrictive energy harvester, and the following characteristics were obtained:

1. The output power of the proposed model is independent of the elastic compliance of the magnetostrictive material.
2. The magnetostrictive energy harvester has an optimal load resistance and capacitance which are independent of the magnetostrictive constant.
3. The optimized harvester with an RC circuit can harvest more output power than that with a pure resistance circuit.

While the proposed model shows a good agreement with experimental data, it requires to precisely estimate the value of magnetostrictive constant and permeability. In principle, these properties can be obtained from measured $S-H$ and $B-H$ curves, respectively, but their values are sensitive to the mechanical and magnetic biases present in the harvester. In particular, the latter may be difficult to estimate analytically due to measurements errors, unknown material properties and manufacturing tolerances. Therefore, the precise measurement and uncertainty analysis must be studied in the future.

CRediT authorship contribution statement

Yoshito Mizukawa: Conceptualization, Methodology, Software, Formal analysis, Resources, Writing – original draft, Writing – review & editing, Funding acquisition. **Umair Ahmed:** Investigation, Writing – review & editing. **Mauro Zucca:** Investigation. **David Blažević:** Writing – review & editing, Supervision, Funding acquisition. **Paavo Rasilo:** Resources, Writing – review & editing, Supervision.

Declaration of competing interest

The authors declare that they have no known competing financial interests or personal relationships that could have appeared to influence the work reported in this paper.

Acknowledgments

The author, Yoshito Mizukawa has received funding from the EDUFI, Finland Fellowship (No. TM-19-11216) and the Finnish Government Scholarship Pool, Finland (No. KM-20-11380) awarded by the Finnish National Agency for Education. David Blažević has received funding from the European Union's Horizon 2020 research and innovation programme under the Marie Skłodowska-Curie grant agreement (No. 838375).

References

[1] S. Roundy, P.K. Wright, J.M. Rabaey, Energy Scavenging for Wireless Sensor Networks, Kluwer Academic Publishers, Boston, USA, 2003.
[2] T. Ueno, Magnetostrictive vibrational power generator for battery-free IoT application, AIP Adv. 9 (3) (2019) http://dx.doi.org/10.1063/1.5079882, 035018.
[3] T. Inoue, Y. Ishida, M. Sumi, Vibration suppression using electromagnetic resonant shunt damper, J. Vib. Acoust. 130 (4) (2008) http://dx.doi.org/10.1115/1.2889916, 041003.
[4] L. Zuo, W. Cui, Dual-functional energy-harvesting and vibration control: Electromagnetic resonant shunt series tuned mass dampers, J. Vib. Acoust. 135 (5) (2013) http://dx.doi.org/10.1115/1.4024095, 051018.
[5] G.K. Ottman, H.F. Hofmann, A.C. Bhatt, G.A. Lesieutre, Adaptive piezoelectric energy harvesting circuit for wireless remote power supply, IEEE Trans. Power Electron. 17 (5) (2002) 669–676, http://dx.doi.org/10.1109/TPEL.2002.802194.
[6] P. Soltani, G. Kerschen, G. Tondreau, A. Deraemaeker, Piezoelectric vibration damping using resonant shunt circuits: an exact solution, Smart Mater. Struct. 23 (12) (2014) 125014, http://dx.doi.org/10.1088/0964-1726/23/12/125014.
[7] J.P. Den Hartog, Mechanical Vibrations, fourth ed., Dover, New York, 1985.
[8] O. Nishihara, T. Asami, Closed-form solutions to the exact optimizations of dynamic vibration absorbers (Minimizations of the maximum amplitude magnification factors), J. Vib. Acoust. 124 (4) (2002) 576–582, http://dx.doi.org/10.1115/1.1500335.
[9] K. Yamada, Enhancing efficiency of piezoelectric element attached to beam using extended spacers, J. Sound Vib. 341 (2015) 31–52, http://dx.doi.org/10.1016/j.jsv.2014.12.022.
[10] T. Ueno, S. Yamada, Performance of energy harvester using Iron–Gallium Alloy in free vibration, IEEE Trans. Magn. 47 (10) (2011) 2407–2409, http://dx.doi.org/10.1109/TMAG.2011.2158303.
[11] A.E. Clark, J.B. Restorff, M. Wun-Fogle, T.A. Lograsso, D.L. Schlagel, Magnetostrictive properties of body-centered cubic Fe-Ga and Fe-Ga-Al alloys, IEEE Trans. Magn. 36 (5) (2000) 3238–3240, http://dx.doi.org/10.1109/20.908752.
[12] R.A. Kellogg, A.B. Flatau, A.E. Clark, M. Wun-Fogle, T.A. Lograsso, Temperature and stress dependencies of the magnetic and magnetostrictive properties of Fe0.81Ga0.19, J. Appl. Phys. 91 (10) (2002) 7821–7823, http://dx.doi.org/10.1063/1.1452216.
[13] J. Atulasimha, A.B. Flatau, A review of magnetostrictive Iron–Gallium alloys, Smart Mater. Struct. 20 (4) (2011) 043001, http://dx.doi.org/10.1088/0964-1726/20/4/043001.
[14] S. Palumbo, P. Rasilo, M. Zucca, Experimental investigation on a Fe-Ga close yoke vibrational harvester by matching magnetic and mechanical biases, J. Magn. Magn. Mater. 469 (2019) 354–363, http://dx.doi.org/10.1016/j.jmmm.2018.08.085.
[15] D. Davino, A. Giustiniani, C. Visone, W. Zamboni, Stress-induced Eddy currents in magnetostrictive energy harvesting devices, IEEE Trans. Magn. 48 (1) (2012) 18–25, http://dx.doi.org/10.1109/TMAG.2011.2162744.
[16] U. Ahmed, J. Jeronen, M. Zucca, S. Palumbo, P. Rasilo, Finite element analysis of magnetostrictive energy harvesting concept device utilizing thermodynamic magneto-mechanical model, J. Magn. Magn. Mater. 486 (2019) 165275, http://dx.doi.org/10.1016/j.jmmm.2019.165275.
[17] U. Ahmed, U. Aydin, M. Zucca, S. Palumbo, R. Kouhia, P. Rasilo, Modeling a fe-ga energy harvester fitted with magnetic closure using 3D magneto-mechanical finite element model, J. Magn. Magn. Mater. 500 (2020) 166390, http://dx.doi.org/10.1016/j.jmmm.2020.166390.
[18] D. Davino, A. Giustiniani, C. Visone, A two-port nonlinear model for magnetoelastic energy-harvesting devices, IEEE Trans. Ind. Electron. 58 (6) (2011) 2556–2564, http://dx.doi.org/10.1109/TIE.2010.2062477.
[19] L. Wang, F.G. Yuan, Vibration energy harvesting by magnetostrictive material, Smart Mater. Struct. 17 (4) (2008) 045009, http://dx.doi.org/10.1088/0964-1726/17/4/045009.
[20] G. Engdahl, Handbook of Giant Magnetostrictive Materials, Academic Press, San Diego, CA, 2000.
[21] C.S. Clemente, A. Mahgoub, D. Davino, C. Visone, Multiphysics circuit of a magnetostrictive energy harvesting device, J. Intell. Mater. Syst. Struct. 28 (17) (2017) 2317–2330, http://dx.doi.org/10.1177/1045389X16685444.
[22] X. Zhao, D.G. Lord, Application of the Villari effect to electric power harvesting, J. Appl. Phys. 99 (8) (2006) 08M703, http://dx.doi.org/10.1063/1.2165133.
[23] J.J. Scheidler, M.J. Dapino, Mechanically induced magnetic diffusion in cylindrical magnetoelastic materials, J. Magn. Magn. Mater. 397 (2016) 233–239, http://dx.doi.org/10.1016/j.jmmm.2015.08.074.
[24] T. Asami, Y. Mizukawa, T. Ise, Optimal design of double-mass dynamic vibration absorbers minimizing the mobility transfer function, J. Vib. Acoust. 140 (6) (2018) http://dx.doi.org/10.1115/1.4040229, 061012.
[25] J.J. Scheidler, V.M. Asnani, M.J. Dapino, Frequency-dependent, dynamic sensing properties of polycrystalline galfenol (Fe81.6Ga18.4), J. Appl. Phys. 119 (24) (2016) 244902, http://dx.doi.org/10.1063/1.4954320.
[26] D. Goll, D. Schuller, G. Martinek, T. Kunert, J. Schurr, C. Sinz, T. Schubert, T. Bernthaler, H. Riegel, G. Schneider, Additive manufacturing of soft magnetic materials and components, Addit. Manuf. (ISSN: 2214-8604) 27 (2019) 428–439, http://dx.doi.org/10.1016/j.addma.2019.02.021.